



Mechanism of Membrane Fusion: Interplay of Lipid and Peptide

Ankita Joardar¹ · Gourab Prasad Pattnaik¹ · Hirak Chakraborty¹

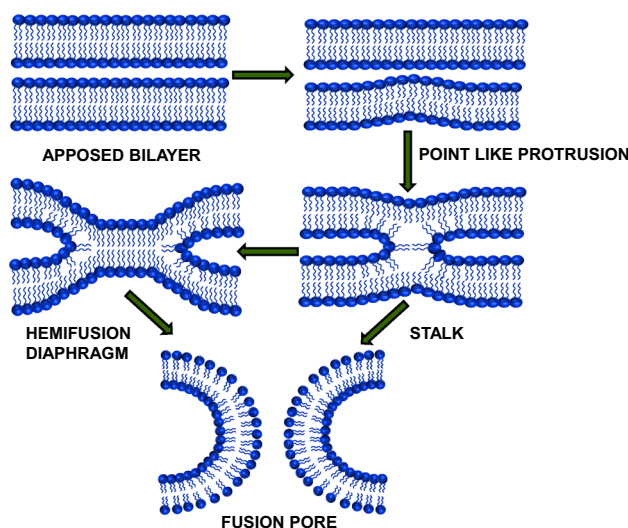
Received: 2 February 2022 / Accepted: 25 March 2022 / Published online: 18 April 2022

© The Author(s), under exclusive licence to Springer Science+Business Media, LLC, part of Springer Nature 2022

Abstract

Membrane fusion is an essential process for the survival of eukaryotes and the entry of enveloped viruses into host cells. A proper understanding of the mechanism of membrane fusion would provide us a handle to manipulate several biological pathways, and design efficient vaccines against emerging and re-emerging viral infections. Although fusion proteins take the central stage in catalyzing the process, role of lipid composition is also of paramount importance. Lipid composition modulates membrane organization and dynamics and impacts the lipid–protein (peptide) interaction. Moreover, the intrinsic curvature of lipids has strong impact on the formation of stalk and hemifusion diaphragm. Detection of transiently stable intermediates remains the bottleneck in the understanding of fusion mechanism. In order to circumvent this challenge, analytical methods can be employed to determine the kinetic parameters from ensemble average measurements of observables, such as lipid mixing, content mixing, and content leakage. The current review aims to present an analytical method that would aid our understanding of the fusion mechanism, provides a better insight into the role of lipid shape, and discusses the interplay of lipid and peptide in membrane fusion.

Graphical Abstract



Keywords Membrane fusion · Lipid stalk model · Intrinsic curvature

Introduction

Membrane fusion is an important process for the survival of eukaryotic systems and entry of enveloped viruses to the host cell (Earp et al. 2005; Jahn et al. 2003; Lucas and Terada

✉ Hirak Chakraborty
hirak@suniv.ac.in; hirakchakraborty@gmail.com

¹ School of Chemistry, Sambalpur University, Jyoti Vihar, Burla, Odisha 768019, India

2004; Mohler et al. 2002). During fusion, two separate lipid bilayers merge into a continuous bilayer and their internal contents get mixed. Membrane fusion mediates a myriad of biological events, such as entry of enveloped viruses into the host cell, fusion of sperm with oocytes (Jahn et al. 2003; Wassarman and Litscher 2008), formation of syncytia of muscle cells (Jahn et al. 2003), transport of newly synthesized membrane constituents like lipids and proteins (Yeagle 2016), endocrine hormone secretion (Aganna et al. 2006), and neuronal signaling (Sollner and Rothman 1994). Moreover, understanding the mechanism of membrane fusion is extremely important to decipher the viral entry mechanism as fusion allows the transfer of viral genome into the host cell. A clear understanding of the process might allow us better handle to develop efficient vaccines and anti-viral therapies (Pattnaik and Chakraborty 2020). This prompted us to understand the membrane fusion process in great detail to control and make it more convenient to lead a healthy life.

Membrane fusion is a common reaction in a biological system that diverges immensely in the area of contact, time, and specific fusogens (Jahn et al. 2003; Mondal Roy and Sarkar 2011). For example, the area of contact for yeast vacuole fusion is about 10,000-fold larger than when synaptic vesicles undergo exocytosis. Further, vacuoles fusion takes time of minute while synaptic vesicle fusion takes place within milliseconds (nearly 10,000-fold shorter than vacuoles fusion) (Jahn et al. 2003). In addition, the fusogens are specific for a specific membrane fusion event (Mondal Roy and Sarkar 2011). Despite the diversity in the fusion reaction, the overall fusion process follows a common route that comprises contact of two membranes (docking), merging of two closely apposed membranes (stalk and transmembrane contact formation), and pore opening for the intermixing of the intracellular material (pore formation) (Chernomordik and Kozlov 2008).

In this review, we have discussed about the lipid stalk model, which is known to be the most accepted fusion mechanism, and how simple ensemble average measurements of certain observables can provide us the detailed information of the fusion process. Further, we have elaborated the effect of lipidic shape and peptide on the fusion mechanism.

Lipid Stalk Hypothesis

Kozlov and Markin gave a preliminary idea on the fusion intermediates in order to understand the mechanism of membrane fusion. Two different models of fusion have been proposed from the concept of fusion intermediates: stalk and adhesion mechanism. According to the stalk mechanism, two approaching membranes form a bridge between them, and the intermediate is termed as ‘stalk.’ The adhesion mechanism suggests the involvement of bilayer reorganization at

the junction of the two bilayers. Adhesion mechanism is further classified as ‘adhesion-micellar mechanism’ and ‘adhesion-condensation mechanism.’ The adhesion-micellar mechanism depicts inverted micellar structure at the merging point of the bilayer, and the adhesion-condensation mechanism involves transition of lipid molecule at the contact region from liquid to crystalline. This crystallization of lipid molecules reduces the area per molecule and generates stress leading to rupture in the external layer of the two approaching liposomes (Kozlov and Markin 1984; Markin et al. 1984). However, the inverted micelle-type intermediate formation is energetically less feasible than the stalk-like intermediate. Micelle-type intermediate forms only under specific conditions close to the transition of bilayer phase into inverse hexagonal (H_{II}) phase and is significantly larger in diameter. Therefore, it involves more lipid molecules than in stalk (Siegel 1993). Consequently, the most accepted hypothesis is stalk intermediate, which was initially conjectured theoretically. However, it has been validated from various numerical simulations (Knecht and Marrink 2007; Marrink and Mark 2003), as the transient intermediates are difficult to visualize experimentally. Two lipid bilayers undergo close apposition by forming a point-like protrusion in one membrane and the other one remains flat (Fig. 1). This point-like protrusion is necessary for minimizing the hydration repulsion of two polar head groups of lipidic membranes connected by surface water (Rand and Parsegian 1989). The hydration repulsion increases exponentially when the flat membrane comes closer to each other because of higher surface area. Therefore, formation of point-like protrusion in one membrane reduces the surface area and hydration repulsion force that meets the approaching surface of the other membrane (Efrat et al. 2007). It is important to mention that the hydration force further depends on the lipid composition (Aeffner et al. 2012; Chakraborty et al. 2014). The point-like protrusion eventually merges with the outer leaflet of the approaching bilayer and forms a continuous structure to acquire a semi-stable hourglass-like intermediate or stalk state. It is known that the lipid membrane transitions from lamellar to hexagonal phase during stalk formation (Siegel and Epanand 1997), and lipids with intrinsic negative curvature facilitates formation of protrusion or bulge, which is essential for formation of stalk intermediate (Akimov et al. 2020). Consequently, the stalk intermediate undergoes radial expansion, and the distal monolayers of two approaching bilayers come closer forming a bilayer by bringing hydrophobic tails of two approaching membranes in contact. This lipidic rearrangement in stalk forms a trilaminar structure known as hemifusion diaphragm, which further undergoes longitudinal expansion to open the pore (Fig. 1).

The intermediate formation requires very high activation energy which is difficult to overcome in the biologically reasonable timescale. The free energy requires for the formation

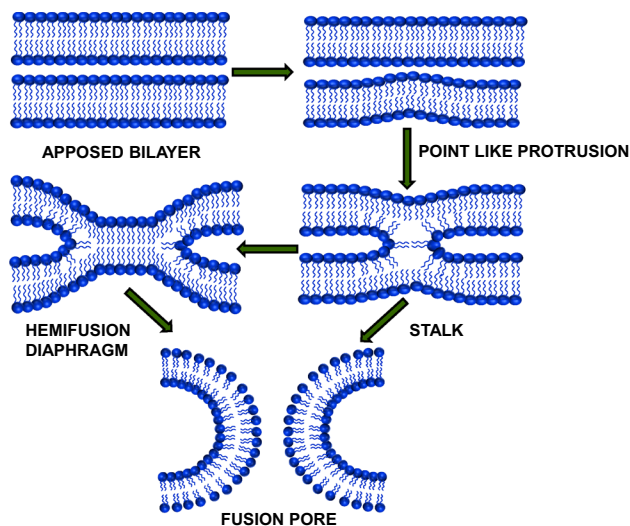


Fig. 1 Schematic representation of intermediate states during membrane fusion according to lipid stalk model

of stalk was based on the energy involved for the bending of monolayer surface (Siegel 1993, 1999). The bending modulus varies with nature of the lipid headgroup, chain length, and chain unsaturation (Rawicz et al. 2000). In stalk state, the inner leaflets (*trans*-monolayer) generate a flat structure while the outer leaflets (*cis*-monolayer) assume curvature. Therefore, interstitial energy generated in the stalk intermediate due to the formation of void within the hydrophobic region where the leaflets are separated. The hydrophobic void was filled by the tilting of lipid tail, and this oblique packing of hydrophobic tails results in a sharp corner in the monolayer (modified stalk) (Hamm and Kozlov 1998, 2000). This generates a curvature in the inner monolayer (*trans*-monolayer) thereby reducing the overall area of stalk. This modulation in the stalk structure was hypothesized by Kozlov's group considering the combined effect of membrane surface bending, splay, and the tilting of hydrocarbon chain. This deformed stalk structure is quite feasible in biological systems due to thermal fluctuations, and it solves the energy crisis of stalk formation (Kozlovsky and Kozlov 2002). Long-chain hydrocarbons are known to fill the void space and stabilize the stalk state. For example, addition of hexadecane into the lipids stabilizes the stalk intermediate and increases the rate of fusion by minimizing the hydrophobic interstitial energy (Chakraborty et al. 2012, 2013; Sengupta et al. 2014). May reported the formation of non-smooth interface at the stalk intermediate, which has a lower free energy compared to the smooth interface (May 2002). The only structural difference between the modified stalk structure and structure given by May is the perpendicular orientation of lipids with respect to the *z*-axis at the junction of stalk. The stalk formation is generally hindered by cone-shaped lipids which generate positive curvature,

and lipids with saturated acyl chain, anionic head group or deprotonated fatty acids (Poojari et al. 2021).

The lateral expansion of stalk structure involves lipidic rearrangement in such a way that the inner leaflets (*trans*-) of two approaching bilayers form another bilayer in their merging point, thereby forming a trilaminar structure. This elongated stalk structure is known as hemifusion diaphragm, which was visualized by confocal fluorescence microscopy (Nikolaus et al. 2010) and cryo-electron microscopy (Hernandez et al. 2012). The stalk structure involves tilting and splay of hydrocarbon chains, and this deformation is responsible for the formation of hemifusion diaphragm (Kozlovsky et al. 2002). The tension generated in the *cis*-leaflets and the presence of excess lipids in the *trans*-leaflet lead to the expansion of stalk (Risselada et al. 2014). The hemifusion diaphragm experiences very high mechanical tension, which prompts pore formation by rupturing the central bilayer. This tension depends on the rim size of the diaphragm or the perimeter of the central bilayer. Molecular dynamic simulation results demonstrated that the metastable hemifusion diaphragm is extremely short-lived and is observed for a few nanoseconds (Knecht and Marrink 2007). The pore size depends on the generated tension on the diaphragm rim; low tension leads to the generation of small or flickering fusion pores, whereas high tension results in large pore opening (Katsov et al. 2004).

The complete fusion requires a productive lateral expansion of hemifusion diaphragm for pore opening. The edge of the pore is longitudinally curved and covered by polar headgroups, which avoids the contact of the hydrophobic interior. Fusion pore formation requires higher activation energy than stalk formation and is controlled by lateral tension generated by proteins or curvature generated by different lipidic shapes. It was observed that positive curvature at the distal leaflet (inner leaflet) is required for pore opening. Therefore, the presence of lipids with positive curvature in the inner leaflet, such as lysophosphatidylcholine, facilitates pore opening (Chernomordik et al. 1995). Small, transient pore formation was also observed at the initial intermediate state(s) (Marrink and Mark 2003). Overall, the fusion process proceeds through the formation of stalk, hemifusion diaphragm, and pore formation.

Determination of Fusion Mechanism from Kinetic Measurements of Observables

As the visualization of fusion intermediates is difficult for their transient nature, it is important to have an analytical model to determine the fusion mechanism from the ensemble-averaged measurements of observables. It was first proposed by Weinreb and Lentz that the parameters pertaining to membrane fusion can be determined from the time courses of

lipid mixing, content mixing, and content leakage using an analytical model (2007). There are fluorescence-based assays to track the time courses of lipid mixing, content mixing, and content leakage. Lipid mixing provides the information of intermixing of lipids between two different vesicles, and this process mainly dominates the stalk and extended transmembrane formation. Content mixing gives us the information of mixing of inner contents of two fusing membranes, and the process mainly occurs during pore formation. However, there is a chance of observing content mixing in early stage of the process as the small fluorophores that are being used for the assay can cross the lipid bilayer of two apposed membranes through thermal fluctuation. Although content leakage does not offer any information of fusion process, it is an important parameter to compensate content mixing signal as it reduces due to occurrence of spontaneous leakage. Moreover, the integrity of the membrane is verified from the content leakage signal.

Lipid Mixing Assay

NBD-PE (donor) and Rh-PE (acceptor) were used for measuring the transfer of lipids (Lipid Mixing) during vesicle fusion and were monitored based on the change in FRET efficiency between FRET lipid pairs (Mondal and Sarkar 2009). FRET dilution as a function of time is considered as a marker to measure the kinetics of lipid transfer (mixing) between two vesicles (Pattnaik and Chakraborty 2021b). It requires to prepare a set of vesicles containing FRET lipid pairs in equal concentration (0.8 mol%), where it shows maximum FRET. The probe-containing vesicles were mixed with probe-free vesicles at a ratio of 1:9 (Chakraborty et al. 2013). The probed lipids will be diluted in the probe-free vesicles during lipid mixing. The kinetics of lipid mixing can be observed as a function of time upon addition of fusogenic agent. Time course of lipid mixing for PEG-induced membrane fusion is shown in Fig. 2A.

Content Mixing Assay

The content mixing can be monitored using the well-established Tb^{3+} and DPA assay proposed by Wilschut and colleagues (1993, 1980). In this assay, vesicles were prepared either in 80 mM DPA or 8 mM $TbCl_3$, and the untrapped DPA and $TbCl_3$ were removed from the external buffer of vesicles using a Sephadex G-75 column equilibrated with assay buffer (10 mM TES, 100 mM NaCl, 1 mM EDTA, 1 mM $CaCl_2$ at pH 7.4). Content mixing within a mixture of 1:1 Tb^{3+} and DPA-containing vesicles was monitored by measuring the increase in fluorescence intensity due to the formation of Tb/DPA complex with time after initiating the mixing process. The change in fluorescence

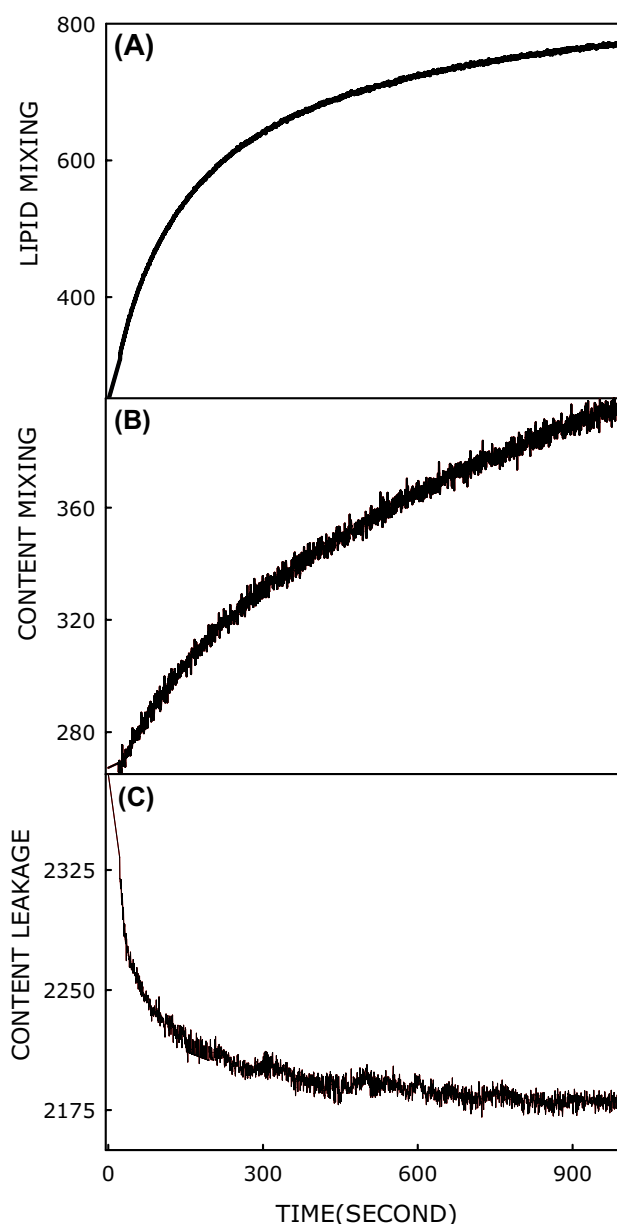
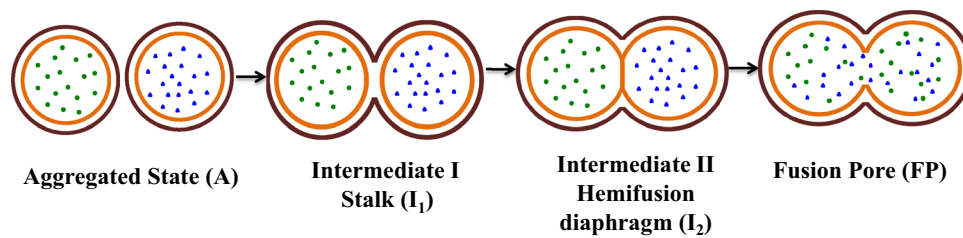


Fig. 2 Representative time courses for **A** lipid mixing, **B** content mixing, and **C** content leakage using the assays mentioned above

intensity due to PEG-induced content mixing as a function of time is shown in Fig. 2B.

Content Leakage Assay

The leakage assay was performed by monitoring the reduction in fluorescence intensity of vesicles containing both $TbCl_3$ and DPA after inducing fusion (Düzgüneş and Wilschut 1993; Wilschut et al. 1980). 8 mM $TbCl_3$ (prepared in 10 mM TES and 100 mM NaCl, pH 7.4) and 80 mM DPA (prepared in 10 mM TES, pH 7.4) were co-encapsulated in vesicles, and the external Tb^{3+}/DPA probe was eliminated



Scheme 1 Schematic representation of membrane fusion process based on lipid stalk model. Aggregated vesicles (A) proceed to fusion pore state (FP) via two-intermediate states (stalk, I_1) and hemifusion diaphragm (I_2). In the analytical modeling of the membrane fusion

process, the states are considered to be thermodynamic states comprising of ensembles of microstructures, which closely resemble to the structures associated with the stalk model of membrane fusion

by running through a Sephadex G-75 column, equilibrated with the assay buffer (10 mM TES, 100 mM NaCl, 1 mM EDTA, 1 mM CaCl_2 , pH 7.4) (Chakraborty et al. 2012). When co-encapsulated Tb^{3+} /DPA complex was discharged from the vesicles, the fluorescence intensity dropped with time due to quenching of Tb^{3+} by EDTA present in the external buffer. Minimum leakage (0%) was characterized by the fluorescence intensity of co-encapsulated Tb /DPA in buffer at zeroth time. The maximum content leakage (100% leakage) was characterized by fluorescence intensity of co-encapsulated TbCl_3 /DPA vesicle treated with detergent such as C_{12}E_8 or Triton X-100. The time course of fluorescence intensity for content leakage during the PEG-induced membrane fusion is shown in Fig. 2C.

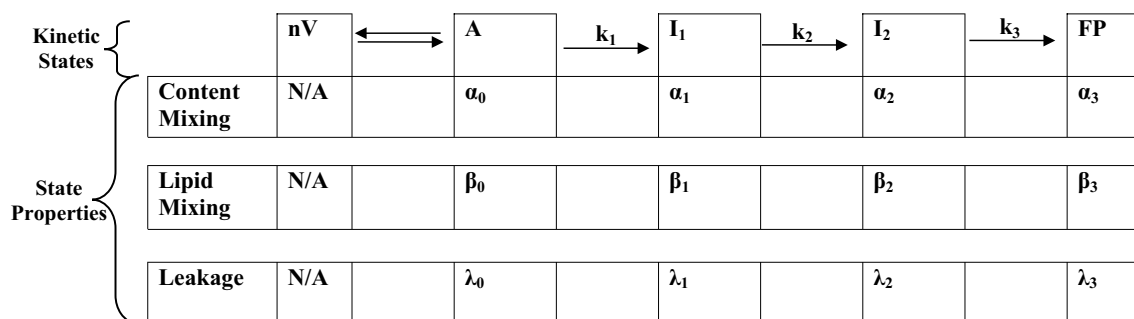
Fusion Model

The proposed kinetic model of membrane fusion is based on the stalk model of fusion, which suggests that individual fusion events proceed through two semi-stable nonlamellar structural intermediates (I_1 and I_2) to form a final fusion pore (Scheme 1) (Chakraborty et al. 2012; Weinreb and Lentz 2007). The states are assumed to be thermodynamic states comprising ensembles of microstructures, which closely resemble the structures associated with the stalk model of membrane fusion. The formalism considers that events related to the content mixing across compartments, leakage of content, and lipid mixing between vesicles occur with finite probabilities in all states (Weinreb and Lentz 2007). The model assumes the occurrence of reversible, small, and flickering pores in the early stage of the process, allowing the movement of contents in osmotically induced fusion of supported bilayers (Chanturiya et al. 1997).

Generally, membrane fusion is considered to proceed through two-intermediate states; however, there are several cases where fusion progresses through single intermediate state (I) (Chakraborty et al. 2013; Weinreb and Lentz 2007). PEG-induced fusion of SUVs containing DOPC/DOPE/SM/CH (35/30/15/20 mol%) proceeds through one-intermediate state in the presence of wild-type hemagglutinin (HA) fusion

peptide from influenza virus (Chakraborty et al. 2013). The single intermediate reaction in the presence of wild-type HA fusion peptide signifies that either I_2 could be destabilized (i.e., I_2 free energy is approximately similar to the energy of the transition state for the formation of I_2 state, allowing I_1 to proceed to the transition state for pore formation without passing through semi-stable I_2 intermediate) or I_1 could evolve without any significant barrier to I_2 , which would then proceed to FP (Chakraborty et al. 2013).

In polyethylene glycol (PEG)-mediated membrane fusion, according to the analytical model, SUVs (nV) rapidly come close to form a thermodynamic state with aggregated vesicles (A). The rate of PEG-mediated aggregation is tenfold higher than the rate of fusion event proposed in the structural model, which avoids the vesicle diffusion event. This aggregated state is further converted to a stalk state (I_1) and hemifusion diaphragm or extended transmembrane contact (I_2) with rate constants k_1 and k_2 , and finally, converted to the fusion pore state with a rate constant k_3 . Every state is expected to be an ensemble of different microclusters and represents the overall kinetic analysis of content leakage (CL), lipid mixing (LM), and content mixing (CM) of any one of the microclusters. The probabilities of LM and CM in each ensemble state are considered as β_i and α_i , respectively, and λ_i is the average rate constant of leakage that occurs in each state (Scheme 2). It is important to mention that all the events are irreversible. The CM and LM probability in the aggregated state (A) are assumed to be zero ($\alpha_0 = \beta_0 = 0$), and at the fusion pore state, CM is predominant over the very negligible lipid mixing ($\beta_3 = 0$). The three independent time courses represented by double exponential could be understood by three intrinsic rate constants (k_1 , k_2 and k_3) and eight extensive parameters (α_1 , α_2 , β_1 , β_2 , λ_0 , λ_1 , λ_2 , λ_3). f_{LM} and f_{CM} have been calculated using the methodology described by Weinreb and Lentz (2007). It would be important to note that the loss of fluorescence signal due to leakage was compensated in the content mixing signal; otherwise, the fraction of content mixing would always be underestimated.



Scheme 2 Schematic representation of the fusion reaction including the rate constants (k_i) of different steps, probabilities of content mixing (α_i) and lipid mixing (β_i), and rate constant of leakage (λ_i) at different states

Weinreb and Lentz had proposed a model that accounts for the time courses of PEG-induced fusion of vesicles utilizing lipid mixing (Fig. 2A), content mixing (Fig. 2B), and content leakage (Fig. 2C) kinetics (2007). The proposed model considered the evolution of fusion pore from aggregated vesicles through either two- or one-intermediate state(s). The mathematical expression for the evolution of fusion states and analytical solutions for the observables (lipid mixing, content mixing, and content leakage) of two-intermediate model have been adopted from the report of Weinreb and Lentz (2007). Expressions for the evolution of states in two-intermediate model are as follows:

$$A(t) = e^{-k_1 t},$$

$$I_1(t) = \frac{k_1}{k_1 - k_2} (e^{-k_2 t} - e^{-k_1 t}),$$

$$I_2(t) = -k_1 k_2 \times \left(\frac{e^{-k_1 t}}{[k_1 - k_2][k_3 - k_1]} + \frac{e^{-k_2 t}}{[k_1 - k_2][k_2 - k_1]} + \frac{e^{-k_3 t}}{[k_2 - k_3][k_3 - k_1]} \right),$$

$$FP(t) = -\frac{k_2 k_3}{[k_1 - k_2][k_3 - k_1]} (1 - e^{-k_1 t}) - \frac{k_1 k_3}{[k_1 - k_2][k_2 - k_3]} (1 - e^{-k_2 t}) - \frac{k_1 k_2}{[k_2 - k_3][k_3 - k_1]} (1 - e^{-k_3 t}).$$

Therefore, by fitting the lipid mixing, content mixing, and content leakage signal utilizing above equations, one can obtain the rate constants for each step. In addition, the probabilities of lipid and content mixing and rate constant of leakage at different states can also be calculated from the analytical model proposed by Weinreb and Lentz (2007) and later modified by Chakraborty et al. (2012). Overall, the analytical model discussed above provides all the descriptors for the fusion reaction to understand the fusion mechanism in detail.

Membrane Curvature: Implications in Membrane Fusion

Lipid composition is an important attributor for membrane fusion as it depends on cell types. Moreover, lipid like cholesterol changes with age. Therefore, it is important to understand the role of lipid composition on membrane fusion. Lipid composition can modulate membrane fusion by altering membrane physical properties, and the structure, organization, and dynamics of fusion proteins and peptides (Meher and Chakraborty 2019). Further, some lipids directly bind to fusion proteins and thereby controlling their fusogenic behavior (Moon and Jun 2020). It has been already discussed that the membrane fusion involves bending of the lipid bilayer to form highly curved intermediates (Chernomordik and Kozlov 2008). Generally, the membrane bending is influenced by several external factors such as

pH, temperature, and salt concentration (Lähdesmäki et al. 2010). In addition, membrane curvature is also affected by the lipid composition (Wang et al. 2007). The headgroup-to-hydrophobic acyl chain length ratio determines the lipid geometry (concave/convex), which has strong influence on membrane curvature (McMahon and Boucrot 2015). Lipids such as phosphatidylethanolamine, cholesterol, and phosphatidic acid having a smaller headgroup-to-hydrophobic acyl chain ratio (inverted cone shaped) induce intrinsic negative

curvature stabilize the stalk intermediate. Conversely, lipids such as phosphatidylinositol, lysophosphatidylcholine, and lysophosphatidic acid having a higher headgroup-to-hydrophobic acyl chain ratio (cones shaped) generate intrinsic positive curvature, and known to inhibit stalk formation (Ashery et al. 2014; Chernomordik and Kozlov 2003; Di Paolo and De Camilli 2006; Furber et al. 2009; Meher and Chakraborty 2019). However, the presence of lipids with intrinsic positive curvature in the inner leaflet facilitates pore formation (Yang et al. 2016a). Therefore, lipid composition has an important role in minimizing the energy requirement for either stalk intermediate or pore formation (Ashery et al. 2014; Furber et al. 2009).

Cholesterol is a vital component of the cell membrane, and it is distributed unevenly in different cell membranes (Colbeau et al. 1971; Lange 1991; Liscum and Underwood 1995; Pattnaik and Chakraborty 2021a; Rothblat et al. 1992). In addition, sphingomyelin regulates the concentration of cholesterol levels in the plasma membrane as it has high affinity toward cholesterol (Liscum and Underwood 1995). The level of cellular cholesterol also varies from person to person, and even with age (Karnell et al. 2005; Martin et al. 2010; Pattnaik and Chakraborty 2019). Cholesterol is known to modulate the organization and dynamics of the membrane (Meher and Chakraborty 2019). Due to the smaller headgroup to the hydrophobic cross-sectional area of the tail, cholesterol induces intrinsic negative curvature to the membrane. Therefore, cholesterol supports the formation of highly curved stalk intermediate and promotes membrane fusion (Aeffner et al. 2012; Pattnaik and Chakraborty 2021a; Yang et al. 2016b). This in turn supports the formation of highly curved intermediate in the course of membrane fusion (Wang et al. 2007). A distinct role of cholesterol has also been established for the entry of many viruses such as the human immunodeficiency virus (HIV) and influenza virus (Pattnaik and Chakraborty 2021a). Moreover, cholesterol is known to promote oligomerization of fusion proteins/peptides to assume fusion competent conformation (Meher et al. 2019). Interestingly, membrane cholesterol affects the inhibitory efficiency of a peptide-based fusion inhibitor TG-23 peptide. It was reported that the inhibitory efficacy of TG-23 diminishes with increasing concentration of membrane cholesterol in the fusion between two membranes having same composition. In addition to the altered peptide dynamics in cholesterol containing membranes, the negative curvature-inducing property of cholesterol might be surpassing the inhibitory effect of TG-23 (Pattnaik and Chakraborty 2019). The asymmetric lipid compositions of the viral envelope and host cell influence the membrane fusion. It is observed that the TG-23 peptide inhibited the fusion between membranes containing 0 and 10 mol% cholesterol, though the efficacy is less than symmetric fusion between membranes devoid of cholesterol, and the inhibitory efficacy becomes

negligible in the fusion between membranes containing 0 and 20 mol% cholesterol. It is demonstrated that the reduction of inhibitory effect of TG-23 in asymmetric membrane fusion containing cholesterol of varying concentrations is not due to the altered peptide structure, organization and dynamics, rather owing to the intrinsic negative curvature-inducing property of cholesterol. Taken together, the negative curvature-inducing property of cholesterol surpasses the inhibitory effect of TG-23 (Pattnaik and Chakraborty 2021b) even in asymmetric membrane fusion.

Phosphatidylethanolamine (PE) is the second most abundant phospholipid after phosphatidylcholine (PC) in mammalian cells (Patel and Witt 2017; van der Veen et al. 2017). The inverted-cone-shaped PE stabilizes the intrinsic negative curvature due to its smaller headgroup size and lower hydration (Damodaran and Merz 1994; McIntosh and Simon 1986; McMahon and Boucrot 2015; McMahon and Gallop 2005; Pink et al. 1998) and, therefore, play a key role in membrane fusion (Emoto and Umeda 2000; Joardar et al. 2021). It has been reported that PE stabilizes the stalk-like intermediate, which eventually proceeds to hemifusion diaphragm and fusion pore formation due to its intrinsic negative curvature (Domanska et al. 2010; Kawamoto et al. 2015; Risselada et al. 2014). However, PE concentration modulates the molecular mechanism of the membrane fusion process. A molecular dynamics study indicates that a high concentration of PE (more than 33 mol%) stabilizes the metastable hemifusion state. Additionally, with a low concentration of PE (such as in the case of 2:1 POPC: POPE), vesicles fuse quickly from the stalk-like state without the formation of an isolated hemifusion diaphragm (Kasson and Pande 2007). A similar experimental observation qualitatively supports that DOPC/DOPE (70/30 mol%) membranes proceed to pore formation through a stalk-like intermediate without the formation of hemifusion diaphragm (Joardar et al. 2021). Measurement of lipid mixing (Fig. 3A), content mixing (Fig. 3B), and content leakage (Fig. 3C) using above-mentioned fluorescence-based methods for the PEG-mediated fusion of DOPC/DOPE (80/20 mol%) and DOPC/DOPE (70/30 mol%), and analyzing them in the analytical method proposed by Weinreb and Lentz (2007) provide the detailed information of the fusion reaction (Table 1). The analysis of data suggested that the fusion of DOPC/DOPE (70/30 mol%) membranes proceeds through a single intermediate state as it was observed for hemagglutinin fusion peptide-induced fusion of DOPC/DOPE/SM/CH (35/30/15/20 mol%) membranes (Chakraborty et al. 2013). It has been observed that the PE drastically enhances the rate of stalk formation, leads the reaction to pore opening. The higher probability of content mixing compared to lipid mixing at the intermediate state further supports that the fusion mechanism circumvents the classical stalk model. The probabilities of lipid mixing and content mixing at different states indicate the chance

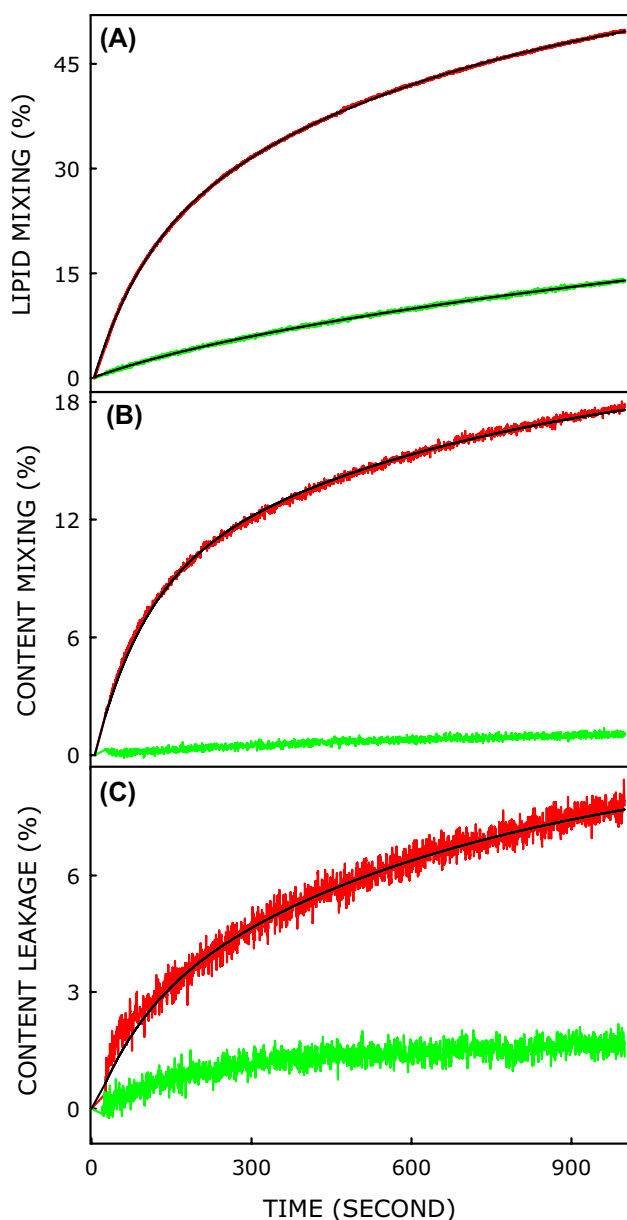


Fig. 3 The kinetics of **A** lipid mixing, **B** content mixing and **C** content leakage in DOPC/DOPE (80/20, mol%) (Green) and DOPC/DOPE (70/30, mol %) (Red), on PEG-mediated SUVs fusion. The membrane fusion was induced by 3% (w/v) of PEG (control) at 37 °C. The black lines are the best fit of the data obtained using one-intermediate model. However, the kinetic data for DOPC/DOPE (80/20 mol%) membranes could not be fitted because of insignificant amount of content mixing. All measurements were carried out in 10 mM TES, 100 mM NaCl, 1 mM CaCl₂ and 1 mM EDTA, pH 7.4 at a total lipid concentration of 200 μM. The representative data is the average of at least three independent measurements. This figure has been adapted from Joardar et al. 2021 with permission

of occurrence of these events during the fusion process. In classical stalk model, it is considered that lipid mixing dominates the early stage whereas content mixing is majorly evident at the later stage of the process. Therefore, it is expected

Table 1 Rate constants of each step, probabilities of lipid and content mixing and rate constants of leakage in each state, and the extent of lipid mixing, content mixing and content leakage of DOPC/DOPE (80/20 mol%) and DOPC/DOPE (70/30 mol%) SUVs

Lipid Composition	$k_1 \times 10^3$ (sec ⁻¹)	$k_3 \times 10^3$ (sec ⁻¹)	α_1	α_3	β_1	β_3	f_{CM}	f_{LM}	$\lambda_0 \times 10^3$ (sec ⁻¹)	$\lambda_1 \times 10^3$ (sec ⁻¹)	$\lambda_3 \times 10^3$ (sec ⁻¹)	R^2
DOPC/DOPE (80/20)	0.62 ± 0.05	NA	NA	NA	0.15 ± 0.02	0.85 ± 0.02	1.4 ± 0.10	21.2 ± 1.06	NA	NA	NA	0.998
DOPC/DOPE (70/30)	11.0 ± 0.06	1.46 ± 0.01	0.48 ± 0.01	0.52 ± 0.01	0.39 ± 0.03	0.61 ± 0.03	21.5 ± 1.05	58.34 ± 2.57	0.09 ± 0.01	0.09 ± 0.01	NA	0.998

The fusion reaction has been triggered by the addition of 3 mol% (w/v) PEG


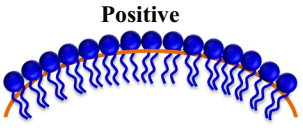

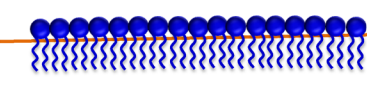

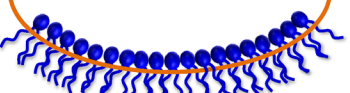
that the value of probability of lipid mixing at the stalk state (β_1) must be higher than the probability of content mixing (α_1). On the other hand, probability of content mixing at the fusion pore state (α_3) is likely to be higher than the probability of lipid mixing (β_3) at this state. Therefore, probabilities of lipid and content mixing could be easily used as a marker for the classical stalk model (Joardar et al. 2021). The results further suggested that the stalk-like intermediate is having properties similar to the fusion pore rather than classical stalk. Altogether, the work provides a complete molecular level information of the fusion of DOPC/DOPE (70/30 mol%) membranes utilizing the analytical model discussed in the review.

Phosphatidic acid (PA) is one of the simplest and minor membrane phospholipids but involves in signaling that regulates several processes in the cell, including cell proliferation, survival, cytoskeletal organization, vesicular trafficking, secretion, reproduction, response to hormones, and abiotic stresses (Zhukovsky et al. 2019). PA typically constitutes 1–4% of membrane lipids. As PA has inverted cone-shaped structure, it promotes intrinsic spontaneous negative curvature in the plasma membrane, thereby facilitating the formation of the highly curved stalk and extended transmembrane contact. The stability of these two intermediates assures the pore formation between two lipid bilayers (Ashery et al. 2014; Chernomordik and Kozlov 2005; Epanand et al. 2015; Meher and Chakraborty 2019) (Fig. 4).

Lysophosphatidylcholine (LPC) displays positive curvature with a curvature radius of +38 to +60 Å whereas lysolipids-containing PE shows negative curvature (−30 Å

(Fuller and Rand 2001). LPC is shown to inhibit hemagglutinin (from influenza virus) fusion peptide-induced fusion (Gunther-Ausborn et al. 1995; Ohki et al. 2006) in a concentration-dependent manner, and gp160-mediated fusion of human immunodeficiency virus (Gunther-Ausborn and Stegmann 1997). LPC further inhibits the Ca^{2+} -, GTP-, and pH-dependent fusion of cell membranes, organelles, and between organelles and plasma membranes (Chernomordik et al. 1993). Stiasny and Heinz observed that the presence of LPC inhibits the low pH-mediated fusion process caused by tick-borne encephalitis virus, a class II flavivirus (2004). The presence of LPC constrained the conversion of lamellar to highly curved nonlamellar phase transition by stabilizing the lamellar structure observed experimentally by ^{31}P nuclear magnetic resonance measurements, and hinder the fusion of Sendai virus (Yeagle et al. 1994). In addition to the alteration of intrinsic membrane curvature, LPC has a strong influence on the membrane organization and dynamics. The presence of LPC at the outer leaflet imparts membrane order both at the interfacial and hydrophobic chain region (Wu et al. 1996). As disordering of the interfacial region is correlated to the ability of stalk formation (Joardar et al. 2021; Pattnaik and Chakraborty 2019; Pattnaik et al. 2018), the increased order at the interfacial region is detrimental to fusion. Oleic acid displays pH-dependent change in intrinsic curvature. At high pH, the deprotonated species assumes intrinsic positive curvature due to higher extent of headgroup hydration (Lähdesmäki et al. 2010). Joardar et al., observed that the oleic acid hinders the rate of intermediate formation, and extent of lipid mixing at the intermediate

Fig. 4 Shape of the phospholipid involves in molecular packing and spontaneous membrane curvature. Schematic representation of lipids with different intrinsic curvature and their impact on the overall membrane curvature

Sl. No.	Shape of the lipid	Curvature	Examples
1	 Conical	 Positive	Lysophosphatidylcholine, Oleic acid, Lysophosphatidic acid
2	 Cylindrical	 Zero	Phosphatidylcholine
3	 Inverted conical	 Negative	Cholesterol, Phosphatidylethanolamine, Phosphatidic acid

at pH 7.4 (2021). The fusion between autophagosome and lysosome is shown to be inhibited by oleic acid (Lee et al. 2019) (Fig. 4).

Peptide-Induced Change in Membrane Curvature: Implications in Membrane Fusion

Lipid bilayers are stable dynamic assemblies that do not fuse naturally but participate in fusion while any fusogen perturbs the organization and dynamics of at least one of the two lipid bilayers, thereby facilitating fusion (Pattnaik et al. 2018). Fusogens affect spontaneous curvature of the membrane in such a way that the activation barrier for stalk, hemifusion diaphragm, or pore formation is reduced to facilitate membrane fusion. Generally, fusion peptides and other molecules that induce negative curvature to the membrane promotes fusion, as a negative curvature in the membrane results in the membrane curving inward and facilitating greater contact area between the two membranes. In contrast, peptides and other molecules that induce positive curvature will inhibit viral fusion, since they will locally curve the membrane outward thereby preventing several contacts between fusion proteins and target membranes (Colotto et al. 1996).

A wide variety of membrane proteins induce membrane curvature for virus-cell fusion. The N-terminal segment of fusion protein, which is critical for viral entry is known as fusion peptide. It is well established that fusion peptide of hemagglutinin (HA) from influenza virus has a strong impact on the virus entry to the host cell. Small-angle X-ray diffraction study indicates that the HA fusion peptide generates a curved lipid structure (cubic) at pH 5.0. Further, it is anticipated that the peptide promotes cubic phases at pH 5.0 by altering the kinetics of the lamellar to inverted phase transitions (Colotto and Epanand 1997). In addition, it is well established that HA fusion peptide promotes negative curvature and, hence, the formation of hexagonal and cubic phases of lipids (Epanand and Epanand 1994; Siegel and Epanand 2000; Tenchov et al. 2013). It was proposed that low pH-induced conformational change of the influenza HA fusion domain employs stress on the lipid bilayer. Han et al., proposed that the deeper insertion of this V-shaped HA fusion peptide increases the lateral pressure within the hydrocarbon area and increases surface tension in the interfacial region of the lipid bilayer. Further, the lipid bilayer may respond to this stress by bending in a concave manner, i.e., by inducing negative curvature that assists the formation of fusion intermediates and completes the process (Han et al. 2001). Smrt et al. have shown that F3G mutant of 23 amino acid residues HA fusion peptide stabilizes the negative curvature less effectively as compared to wild-type hemagglutinin fusion peptide (HAfp23) that results in decreased fusogenicity of the former with respect to later (2015).

SIVwt, and SIVmutV, are two different peptides that resemble the N-terminus of the simian immunodeficiency virus (SIV) glycoprotein gp32, have the same amino acid composition, and hence, hydrophobicity, but altered amino acid sequences. The SIVwt peptide inserts into the membrane at an oblique angle to the membrane normal (Martin et al. 1991), whereas SIVmutV inserts into the membrane perpendicular to the plane of the bilayer (Martin et al. 1994). X-ray diffraction study reveals that both peptides have a bilayer destabilizing effect. Interestingly, SIVwt destabilizes the bilayer by inducing a negative curvature, whereas SIVmutV peptide destabilizes the bilayer by inducing a positive curvature resulting the wild-type peptide to promote fusion whereas the mutant inhibits it (Colotto et al. 1996).

Using solid-state NMR spectroscopy, the interactions of the fusion peptide of the paramyxovirus (PIV5) in three different lipid membranes, POPC/POPG, DOPC/DOPG, and DOPE were studied. It has been observed that the peptide assumes α -helical in the POPC/POPG membrane, a mixed strand/helix conformation in the DOPC/DOPG membrane, and mostly a β -strand in the DOPE membrane. Interestingly, ^{31}P NMR spectra showed that the peptide retains the lamellar structure and hydration of POPC/POPG, DOPC/DOPG membranes. However, the fusion peptide dehydrates the DOPE membrane and destabilizes its inverted hexagonal phase to assume cubic phase. It has been hypothesized that the β -strand conformation of the fusion peptide generates negative Gaussian curvature, and dehydration of DOPE membrane might be crucial for hemifusion intermediate formation in order to promote membrane fusion (Yao and Hong 2014).

Unlike other class-I viruses, spike protein (S-protein) of severe acute respiratory syndrome coronaviruses (SARS-CoVs) contain multiple peptide sequences that are instrumental in their entry into the host cell. In addition to the classical N-terminal fusion peptide (FP), S-protein contains internal fusion peptides (IFPs), and a segment located upstream of the transmembrane domain known as pre-transmembrane domain (PTM) (Chakraborty and Bhattacharjya 2020). Interestingly, there is decent amount of sequence homology between fusion peptides of SARS-CoV-1 and SARS-CoV-2 (Pattnaik et al. 2021). Guillén et al., proposed a model involving the participation of three membranotropic peptides of S-protein in a synergistic way to induce fusion. In this model, insertion of FP into the host cell leads to the formation of the pre-hairpin intermediate followed by refolding of HR1 and HR2 and formation of six-helix bundle. Subsequently, the juxtaposition of IFP and PTM facilitates the hemifusion formation. These two regions could also facilitate the formation of fusion pore through lipid destabilization at the late steps of the membrane fusion process (Guillén et al. 2008). It has been demonstrated that cholesterol-dependent enhancement of IFP and FP-induced

hemifusion formation. Cholesterol-dependent enhancement could be attributed to the changes in the physical properties of the membrane including the intrinsic negative curvature (Pattnaik et al. 2021). The inverted cone-like structure of cholesterol generates intrinsic negative curvature to the membrane and facilitates formation of nonlamellar fusion intermediate. Overall, membrane composition plays a crucial role in the entry of SARS-CoV as it alters organization, dynamics, and conformation of the fusion peptide as well as the membrane organization and dynamics (Basso et al. 2016; Chakraborty and Bhattacharjya 2020). Using differential scanning calorimetry, Basso et al., observed that FP induces positive curvature on DiPoPE vesicles, whereas IFP promotes opposing stresses on the intrinsic negative curvature of DiPoPE depending on the ionic strength. Further, using electron spin resonance spectroscopy, they demonstrated that fusion peptides increase lipid packing, and head-group ordering and reduce the intramembrane water content for anionic membranes. This leads to generating bending moment in the bilayer and promoting negative curvature. The collective effect of SARS-CoV fusion peptides on the membrane physical properties reduces the activation barrier required during the SARS-CoV-induced membrane fusion (Basso et al. 2016).

Concluding Remarks

Understanding the mechanism of membrane fusion is essential to understand several biological processes and develop efficient vaccines and therapies against emerging and re-emerging viral diseases. The major challenge in understanding the mechanism is to visualize the fusion intermediates due to their transient existence. In this review, we have discussed an analytical method to determine the fusion mechanism from the fluorescence-based ensemble averaged measurements of lipid mixing, content mixing, and content leakage. In addition, we have discussed about the effect of lipidic shape on membrane curvature, and the importance of lipid-peptide interaction in understanding the peptide-catalyzed membrane fusion. Overall, the review provides a detailed molecular level information of membrane fusion, which might be useful for designing efficient fusion inhibitors.

Acknowledgements This work was supported by research grant from the Science and Technology Department, Government of Odisha. H.C. thanks the University Grants Commission for UGC-Assistant Professor position. A.J. and G.P.P. acknowledge Science and Technology Department, Government of Odisha, and Council of Scientific and Industrial Research for Senior Research Fellowship, respectively. We thank members of Chakraborty laboratory for their comments and discussions.

Funding The study was funded by Science and Technology Department, Government of Odisha.

Declarations

Conflict of interest The authors declare that there is no conflict of interest.

References

- Aeffner S, Reusch T, Weinhausen B, Salditt T (2012) Energetics of stalk intermediates in membrane fusion are controlled by lipid composition. *Proc Natl Acad Sci USA* 109:E1609–1618
- Aganna E, Burrin JM, Hitman GA, Turner MD (2006) Involvement of calpain and synaptotagmin Ca^{2+} sensors in hormone secretion from excitable endocrine cells. *J Endocrinol* 190:R1–7
- Akimov SA, Molotkovsky RJ, Kuzmin PI, Galimzyanov TR, Batishchev OV (2020) Continuum models of membrane fusion: evolution of the theory. *Int J Mol Sci* 21:3875
- Ashery U, Bielopolski N, Lavi A, Barak B, Michaeli L, Ben-Simon Y, Sheinin A, Bar-On D, Shapira Z, Gottfried I (2014) The molecular mechanisms underlying synaptic transmission: a view of the presynaptic terminal. In: Pickel V, Segal M (eds) *The synapse*. Academic Press, Boston, pp 21–109
- Basso LG, Vicente EF, Crusca E Jr, Cilli EM, Costa-Filho AJ (2016) SARS-CoV fusion peptides induce membrane surface ordering and curvature. *Sci Rep* 6:37131
- Chakraborty H, Bhattacharjya S (2020) Mechanistic insights of host cell fusion of SARS-CoV-1 and SARS-CoV-2 from atomic resolution structure and membrane dynamics. *Biophys Chem* 265:106438
- Chakraborty H, Tarafdar PK, Bruno MJ, Sengupta T, Lentz BR (2012) Activation thermodynamics of poly(ethylene glycol)-mediated model membrane fusion support mechanistic models of stalk and pore formation. *Biophys J* 102:2751–2760
- Chakraborty H, Tarafdar PK, Klapper DG, Lentz BR (2013) Wild-type and mutant hemagglutinin fusion peptides alter bilayer structure as well as kinetics and activation thermodynamics of stalk and pore formation differently: mechanistic implications. *Biophys J* 105:2495–2506
- Chakraborty H, Sengupta T, Lentz BR (2014) pH Alters PEG-mediated fusion of phosphatidylethanolamine-containing vesicles. *Biophys J* 107:1327–1238
- Chanturiya A, Chernomordik LV, Zimmerberg J (1997) Flickering fusion pores comparable with initial exocytotic pores occur in protein-free phospholipid bilayers. *Proc Natl Acad Sci USA* 94:14423–14428
- Chernomordik LV, Kozlov MM (2003) Protein-lipid interplay in fusion and fission of biological membranes. *Annu Rev Biochem* 72:175–207
- Chernomordik LV, Kozlov MM (2005) Membrane hemifusion: crossing a chasm in two leaps. *Cell* 123:375–382
- Chernomordik LV, Kozlov MM (2008) Mechanics of membrane fusion. *Nat Struct Mol Biol* 15:675–683
- Chernomordik LV, Vogel SS, Sokoloff AV, Onaran HO, Leikina E, Zimmerberg J (1993) Lysolipids reversibly inhibit Ca^{2+} , GTP and pH dependent fusion of biological membranes. *FEBS Lett* 318:71–76
- Chernomordik L, Chanturiya A, Green J, Zimmerberg J (1995) The hemifusion intermediate and its conversion to complete fusion: regulation by membrane composition. *Biophys J* 69:922–929

- Colbeau A, Nachbaur J, Vignais PM (1971) Enzymic characterization and lipid composition of rat liver subcellular membranes. *Biochim Biophys Acta* 249:462–492
- Colotto A, Epand RM (1997) Structural study of the relationship between the rate of membrane fusion and the ability of the fusion peptide of influenza virus to perturb bilayers. *Biochemistry* 36:7644–7651
- Colotto A, Martin I, Ruyschaert JM, Sen A, Hui SW, Epand RM (1996) Structural study of the interaction between the SIV fusion peptide and model membranes. *Biochemistry* 35:980–989
- Damodaran KV, Merz KM Jr. (1994) A comparison of DMPC- and DLPE-based lipid bilayers. *Biophys J* 66:1076–1087
- Di Paolo G, De Camilli P (2006) Phosphoinositides in cell regulation and membrane dynamics. *Nature* 443:651–657
- Domanska MK, Kiessling V, Tamm LK (2010) Docking and fast fusion of synaptobrevin vesicles depends on the lipid compositions of the vesicle and the acceptor SNARE complex-containing target membrane. *Biophys J* 99:2936–2946
- Düzgüneş N, Wilschut J (1993) Fusion assays monitoring intermixing of aqueous contents. *Methods Enzymol* 220:3
- Earp LJ, Delos SE, Park HE, White JM (2005) The many mechanisms of viral membrane fusion proteins. *Curr Top Microbiol Immunol* 285:25–66
- Efrat A, Chernomordik LV, Kozlov MM (2007) Point-like protrusion as a prestalk intermediate in membrane fusion pathway. *Biophys J* 92:L61–63
- Emoto K, Umeda M (2000) An essential role for a membrane lipid in cytokinesis. Regulation of contractile ring disassembly by redistribution of phosphatidylethanolamine. *J Cell Biol* 149:1215–1224
- Epand RM, Epand RF (1994) Relationship between the infectivity of influenza virus and the ability of its fusion peptide to perturb bilayers. *Biochem Biophys Res Commun* 202:1420–1425
- Epand RM, D'Souza K, Berno B, Schlame M (2015) Membrane curvature modulation of protein activity determined by NMR. *Biochim Biophys Acta Biomembr* 1848:220–228
- Fuller N, Rand RP (2001) The influence of lysolipids on the spontaneous curvature and bending elasticity of phospholipid membranes. *Biophys J* 81:243–254
- Furber KL, Churchward MA, Rogasevskaia TP, Coorssen JR (2009) Identifying critical components of native Ca²⁺-triggered membrane fusion. Integrating studies of proteins and lipids. *Ann N Y Acad Sci* 1152:121–134
- Guillén J, Kinnunen PK, Villalán J (2008) Membrane insertion of the three main membranotropic sequences from SARS-CoV S2 glycoprotein. *Biochim Biophys Acta* 1778:2765–2774
- Gunther-Ausborn S, Stegmann T (1997) How lysophosphatidylcholine inhibits cell-cell fusion mediated by the envelope glycoprotein of human immunodeficiency virus. *Virology* 235:201–208
- Gunther-Ausborn S, Praetor A, Stegmann T (1995) Inhibition of influenza-induced membrane fusion by lysophosphatidylcholine. *J Biol Chem* 270:29279–29285
- Hamm M, Kozlov MM (1998) Tilt model of inverted amphiphilic mesophases. *Eur Phys J B* 6:519–528
- Hamm M, Kozlov MM (2000) Elastic energy of tilt and bending of fluid membranes. *Eur Phys J E* 3:323–335
- Han X, Bushweller JH, Cafiso DS, Tamm LK (2001) Membrane structure and fusion-triggering conformational change of the fusion domain from influenza hemagglutinin. *Nat Struct Biol* 8:715–720
- Hernandez JM, Stein A, Behrmann E, Riedel D, Cypionka A, Farsi Z, Walla PJ, Raunser S, Jahn R (2012) Membrane fusion intermediates via directional and full assembly of the SNARE complex. *Science* 336:1581–1584
- Jahn R, Lang T, Sudhof TC (2003) Membrane fusion. *Cell* 112:519–533
- Joardar A, Pattnaik GP, Chakraborty H (2021) Effect of phosphatidylethanolamine and oleic acid on membrane fusion: phosphatidylethanolamine circumvents the classical stalk model. *J Phys Chem B* 125:13192–13202
- Karnell FG, Brezski RJ, King LB, Silverman MA, Monroe JG (2005) Membrane cholesterol content accounts for developmental differences in surface B cell receptor compartmentalization and signaling. *J Biol Chem* 280:25621–25628
- Kasson PM, Pande VS (2007) Control of membrane fusion mechanism by lipid composition: predictions from ensemble molecular dynamics. *PLoS Comput Biol* 3:e220
- Katsov K, Muller M, Schick M (2004) Field theoretic study of bilayer membrane fusion. I. Hemifusion mechanism. *Biophys J* 87:3277–3290
- Kawamoto S, Klein ML, Shinoda W (2015) Coarse-grained molecular dynamics study of membrane fusion: curvature effects on free energy barriers along the stalk mechanism. *J Chem Phys* 143:243112
- Knecht V, Marrink SJ (2007) Molecular dynamics simulations of lipid vesicle fusion in atomic detail. *Biophys J* 92:4254–4261
- Kozlov MM, Markin VS (1984) On the theory of membrane fusion. The adhesion-condensation mechanism. *Gen Physiol Biophys* 3:379–402
- Kozlovsky Y, Kozlov MM (2002) Stalk model of membrane fusion: solution of energy crisis. *Biophys J* 82:882–895
- Kozlovsky Y, Chernomordik LV, Kozlov MM (2002) Lipid intermediates in membrane fusion: formation, structure, and decay of hemifusion diaphragm. *Biophys J* 83:2634–2651
- Lähdesmäki K, Ollila OHS, Koivuniemi A, Kovanen PT, Hyvönen MT (2010) Membrane simulations mimicking acidic pH reveal increased thickness and negative curvature in a bilayer consisting of lysophosphatidylcholines and free fatty acids. *Biochim Biophys Biomembr* 1798:938–946
- Lange Y (1991) Disposition of intracellular cholesterol in human fibroblasts. *J Lipid Res* 32:329–339
- Lee DH, Ahn J, Jang YJ, Ha TY, Jung CH (2019) Oleic acid-induced defective autolysosome shows impaired lipid degradation. *Biochem Biophys Res Commun* 513:553
- Liscum L, Underwood KW (1995) Intracellular cholesterol transport and compartmentation. *J Biol Chem* 270:15443–15446
- Lucas JJ, Terada N (2004) Spontaneous cell fusion. In: Lanza R, Gearhart J, Hogan B, Melton D, Pedersen R, Thomson J, West M (eds) *Handbook of stem cells*. Academic Press, Burlington, pp 153–158
- Markin VS, Kozlov MM, Borovjagin VL (1984) On the theory of membrane fusion. The stalk mechanism. *Gen Physiol Biophys* 3:361–377
- Marrink SJ, Mark AE (2003) The mechanism of vesicle fusion as revealed by molecular dynamics simulations. *J Am Chem Soc* 125:11144–11145
- Martin I, Defrise-Quertain F, Mandieau V, Nielsen NM, Saermark T, Burny A, Brasseur R, Ruyschaert JM, Vandenbranden M (1991) Fusogenic activity of SIV (simian immunodeficiency virus) peptides located in the GP32 NH2 terminal domain. *Biochem Biophys Res Commun* 175:872–879
- Martin I, Dubois MC, Defrise-Quertain F, Saermark T, Burny A, Brasseur R, Ruyschaert JM (1994) Correlation between fusogenicity of synthetic modified peptides corresponding to the NH2-terminal extremity of simian immunodeficiency virus gp32 and their mode of insertion into the lipid bilayer: an infrared spectroscopy study. *J Virol* 68:1139–1148
- Martin M, Dotti CG, Ledesma MD (2010) Brain cholesterol in normal and pathological aging. *Biochim Biophys Acta* 1801:934–944

- May S (2002) Structure and energy of fusion stalks: the role of membrane edges. *Biophys J* 83:2969–2980
- McIntosh TJ, Simon SA (1986) Area per molecule and distribution of water in fully hydrated dilauroylphosphatidylethanolamine bilayers. *Biochemistry* 25:4948–4952
- McMahon HT, Boucrot E (2015) Membrane curvature at a glance. *J Cell Sci* 128:1065–1070
- McMahon HT, Gallop JL (2005) Membrane curvature and mechanisms of dynamic cell membrane remodelling. *Nature* 438:590–596
- Meher G, Chakraborty H (2019) Membrane composition modulates fusion by altering membrane properties and fusion peptide structure. *J Membr Biol* 252:261–272
- Meher G, Bhattacharjya S, Chakraborty H (2019) Membrane cholesterol modulates oligomeric status and peptide-membrane interaction of severe acute respiratory syndrome coronavirus fusion peptide. *J Phys Chem B* 123:10654–10662
- Mohler WA, Shemer G, del Campo JJ, Valansi C, Opoku-Serebuoh E, Scranton V, Assaf N, White JG, Podbilewicz B (2002) The type I membrane protein EFF-1 is essential for developmental cell fusion. *Dev Cell* 2:355–362
- Mondal Roy S, Sarkar M (2011) Membrane fusion induced by small molecules and ions. *J Lipids* 2011:528784
- Mondal S, Sarkar M (2009) Non-steroidal anti-inflammatory drug induced membrane fusion: concentration and temperature effects. *J Phys Chem B* 113:16323–16332
- Moon Y, Jun Y (2020) The effects of regulatory lipids on intracellular membrane fusion mediated by dynamin-like GTPases. *Front Cell Dev Biol* 8:518
- Nikolaus J, Stockl M, Langosch D, Volkmer R, Herrmann A (2010) Direct visualization of large and protein-free hemifusion diaphragms. *Biophys J* 98:1192–1199
- Ohki S, Baker GA, Page PM, McCarty TA, Epanand RM, Bright FV (2006) Interaction of influenza virus fusion peptide with lipid membranes: effect of lysolipid. *J Membr Biol* 211:191–200
- Patel D, Witt SN (2017) Ethanolamine and phosphatidylethanolamine: partners in health and disease. *Oxid Med Cell Longev* 2017:4829180
- Pattanaik GP, Chakraborty H (2019) Cholesterol alters the inhibitory efficiency of peptide-based membrane fusion inhibitor. *Biochim Biophys Acta Biomembr* 1861:183056
- Pattanaik GP, Chakraborty H (2020) Entry inhibitors: efficient means to block viral infection. *J Membr Biol* 253:425–444
- Pattanaik GP, Chakraborty H (2021a) Cholesterol: a key player in membrane fusion that modulates the efficacy of fusion inhibitor peptides. *Vitam Horm* 117:133–155
- Pattanaik GP, Chakraborty H (2021b) Fusogenic effect of cholesterol prevails over the inhibitory effect of a peptide-based membrane fusion inhibitor. *Langmuir* 37:3477–3489
- Pattanaik GP, Meher G, Chakraborty H (2018) Exploring the mechanism of viral peptide-induced membrane fusion. *Adv Exp Med Biol* 1112:69–78
- Pattanaik GP, Bhattacharjya S, Chakraborty H (2021) Enhanced cholesterol-dependent hemifusion by internal fusion peptide 1 of SARS coronavirus-2 compared to its N-terminal counterpart. *Biochemistry* 60:559–562
- Pink DA, McNeil S, Quinn B, Zuckermann MJ (1998) A model of hydrogen bond formation in phosphatidylethanolamine bilayers. *Biochim Biophys Acta* 1368:289–305
- Poojari CS, Scherer KC, Hub JS (2021) Free energies of membrane stalk formation from a lipidomics perspective. *Nat Commun* 12:6594
- Rand RP, Parsegian VA (1989) Hydration forces between phospholipid bilayers. *Biochim Biophys Acta Biomembr* 988:351–376
- Rawicz W, Olbrich KC, McIntosh T, Needham D, Evans E (2000) Effect of chain length and unsaturation on elasticity of lipid bilayers. *Biophys J* 79:328–339
- Risselada HJ, Bubnis G, Grubmuller H (2014) Expansion of the fusion stalk and its implication for biological membrane fusion. *Proc Natl Acad Sci USA* 111:11043–11048
- Rothblat GH, Mahlberg FH, Johnson WJ, Phillips MC (1992) Apolipoproteins, membrane cholesterol domains, and the regulation of cholesterol efflux. *J Lipid Res* 33:1091–1097
- Sengupta T, Chakraborty H, Lentz BR (2014) The transmembrane domain peptide of vesicular stomatitis virus promotes both intermediate and pore formation during PEG-mediated vesicle fusion. *Biophys J* 107:1318–1326
- Siegel DP (1993) Energetics of intermediates in membrane fusion: comparison of stalk and inverted micellar intermediate mechanisms. *Biophys J* 65:2124–2140
- Siegel DP (1999) The modified stalk mechanism of lamellar/inverted phase transitions and its implications for membrane fusion. *Biophys J* 76:291–313
- Siegel DP, Epanand RM (1997) The mechanism of lamellar-to-inverted hexagonal phase transitions in phosphatidylethanolamine: implications for membrane fusion mechanisms. *Biophys J* 73:3089–3111
- Siegel DP, Epanand RM (2000) Effect of influenza hemagglutinin fusion peptide on lamellar/inverted phase transitions in dipalmitoleoylphosphatidylethanolamine: implications for membrane fusion mechanisms. *Biochim Biophys Acta* 1468:87–98
- Smrt ST, Draney AW, Lorieau JL (2015) The influenza hemagglutinin fusion domain is an amphipathic helical hairpin that functions by inducing membrane curvature. *J Biol Chem* 290:228–238
- Sollner T, Rothman JE (1994) Neurotransmission: harnessing fusion machinery at the synapse. *Trends Neurosci* 17:344–348
- Stiasny K, Heinz FX (2004) Effect of membrane curvature-modifying lipids on membrane fusion by tick-borne encephalitis virus. *J Virol* 78:8536–8542
- Tenchov BG, MacDonald RC, Lentz BR (2013) Fusion peptides promote formation of bilayer cubic phases in lipid dispersions. An X-ray diffraction study. *Biophys J* 104:1029–1037
- van der Veen JN, Kennelly JP, Wan S, Vance JE, Vance DE, Jacobs RL (2017) The critical role of phosphatidylcholine and phosphatidylethanolamine metabolism in health and disease. *Biochim Biophys Acta Biomembr* 1859:1558–1572
- Wang W, Yang L, Huang HW (2007) Evidence of cholesterol accumulated in high curvature regions: implication to the curvature elastic energy for lipid mixtures. *Biophys J* 92:2819–2830
- Wassarman PM, Litscher ES (2008) Mammalian fertilization is dependent on multiple membrane fusion events. *Methods Mol Biol* 475:99–113
- Weinreb G, Lentz BR (2007) Analysis of membrane fusion as a two-state sequential process: evaluation of the stalk model. *Biophys J* 92:4012–4029
- Wilschut J, Duzgunes N, Fraley R, Papahadjopoulos D (1980) Studies on the mechanism of membrane fusion: kinetics of calcium ion induced fusion of phosphatidylserine vesicles followed by a new assay for mixing of aqueous vesicle contents. *Biochemistry* 19:6011–6021
- Wu H, Zheng L, Lentz BR (1996) A slight asymmetry in the transbilayer distribution of lysophosphatidylcholine alters the surface properties and poly(ethylene glycol)-mediated fusion of dipalmitoylphosphatidylcholine large unilamellar vesicles. *Biochemistry* 35:12602–12611
- Yang ST, Kiessling V, Tamm LK (2016a) Line tension at lipid phase boundaries as driving force for HIV fusion peptide-mediated fusion. *Nat Commun* 7:11401
- Yang ST, Kreutzberger AJB, Lee J, Kiessling V, Tamm LK (2016b) The role of cholesterol in membrane fusion. *Chem Phys Lipids* 199:136–143
- Yao H, Hong M (2014) Conformation and lipid interaction of the fusion peptide of the paramyxovirus PIV5 in anionic and

- negative-curvature membranes from solid-state NMR. *J Am Chem Soc* 136:2611–2624
- Yeagle PL (2016) Membrane fusion. In: Yeagle PL (ed) *The membranes of cells*, 3rd edn. Academic Press, Boston, pp 379–399
- Yeagle PL, Smith FT, Young JE, Flanagan TD (1994) Inhibition of membrane fusion by lysophosphatidylcholine. *Biochemistry* 33:1820–1827
- Zhukovsky MA, Filograna A, Luini A, Corda D, Valente C (2019) Phosphatidic acid in membrane rearrangements. *FEBS Lett* 593:2428–2451

Publisher's Note Springer Nature remains neutral with regard to jurisdictional claims in published maps and institutional affiliations.